Improving Performance of High Speed GaN Transistors Operating in Parallel for High Current Applications

David Reusch and Johan Strydom
Efficient Power Conversion Corporation (EPC), El Segundo, CA, USA.
David.Reusch@epc-co.com

Abstract

The emergence of gallium nitride (GaN) based power devices offers the potential to achieve higher efficiencies and higher switching frequencies than possible with silicon (Si) power MOSFETs. In this paper, we will evaluate the ability to parallel high speed GaN transistors in applications requiring higher output current. The impact of in-circuit parasitics on performance will be assessed and a PCB layout technique will be proposed to improve the performance of high speed GaN transistors operating in parallel. Four parallel half bridges in an optimized layout operated as a 48 V to 12 V, 480 W, 300 kHz, 40 A single phase buck converter achieving efficiencies above 96.5% from 35% to 100% load will be demonstrated.

1. Introduction

As technology evolves and advances, the system power demands also become more complex. Power converters are constantly trending towards higher output power, higher efficiency, higher power density, higher temperature operation, and higher reliability, all while providing a lower overall system cost. To provide improved performance better power devices are required. For silicon (Si) power devices, the gains in performance have slowed as the technology has matured and approaches its theoretical limits [1]. Gallium nitride (GaN) transistors have emerged as a possible replacement for silicon devices in various power conversion applications. GaN transistors are high electron mobility transistors (HEMT) with a higher band gap, critical electric field strength, and electron mobility than silicon devices [1,2]. These material characteristics make the GaN transistor more suitable for higher frequencies.

In this paper, we will compare the critical parameters of GaN and Si devices that impact performance in hard-switching power converters, discuss the impact of parasitics on performance, including both package and printed circuit board (PCB) layout parasitics, and then evaluate the ability to parallel high speed GaN transistors for higher power applications. A method to improve the parallel performance of GaN transistors will be proposed and experimentally verified for four parallel half bridges operated as a 48 V to 12 V, 480 W, 300 kHz, 40 A single phase buck converter.

2. Comparing Performance Metrics of GaN and Si Power Devices

The first commercially available enhancement mode gallium nitride transistors have a lateral structure with voltages ranging from 40-200 V. These HEMT transistors operate similarly to traditional Si MOSFETs [1,3,4] and their ability to improve in-circuit performance can be evaluated by considering a traditional hard-switching transition as shown in Fig. 1. The switching losses are impacted primarily by two device parameters, Q_{GD}, the gate-to-drain charge, which controls the voltage rising (t_{VR}) and falling transition times; and Q_{GS2}, which is the portion of the gate-to-source charge from the device threshold voltage to the gate plateau voltage, which controls the current rising and falling transition times (t_{CF}).

The power loss during the turn-on and turn-off switching transitions can be given by:

$$P_{SW} = \frac{V_{IN} \cdot I_{OUT} \cdot (Q_{GD} + Q_{GS2})}{I_G} \cdot f_{sw} \quad (1)$$

Where V_{IN} is the input voltage, I_{OUT} is the output current, Q_{GD} is the voltage-dependent gate-to-drain charge, Q_{GS2} is the load current-dependent gate-to-source charge, I_G is the gate driver current, and f_{sw} is the switching frequency.

A figure of merit (FOM), which is a useful tool to compare the in-circuit performance capability of a given device technology [5]-[7], can be derived by combining the dynamic switching loss from equation (1) and the static conduction losses. A hard-switching FOM suitable for low voltage GaN transistors is given by [7]:

$$FOM_{HS} = (Q_{GD} + Q_{GS2}) \cdot R_{DS(on)} \quad (2)$$

Where $R_{DS(on)}$ is the on-resistance of the device.

For a given technology, a lower value of FOM will be able to reduce the total power loss of the device proportional to:

$$P_{LOSS} \propto \sqrt{FOM_{HS}} \quad (3)$$

The comparison of hard-switching FOM for a 100 V eGaN FET and 100 V state of the art MOSFETs is shown in Fig. 1. The eGaN FET FOM is around 25% of the best state of the art Si MOSFET. From equation (3), the reduction in FOM translates into a 50% lower device loss by replacing Si MOSFETs with eGaN FETs.

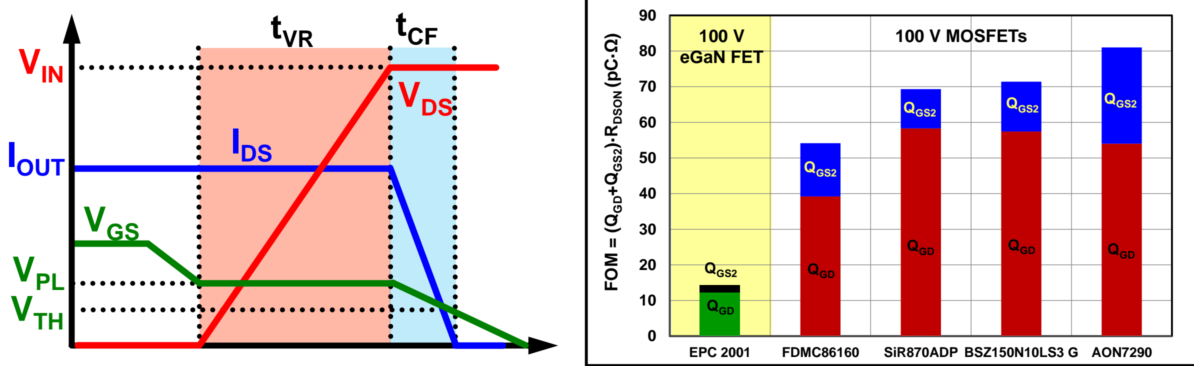

Fig. 1. Ideal hard-switching waveforms for turn-off transition and 100 V device figure of merit comparison (V_{DS}=50 V, I_{DS}=10 A).

3. Impacts of Parasitics on Performance

In practical applications, FOM is just one of the contributors to achieving higher efficiency. In a buck converter, there are two major parasitic inductances that have a significant impact on converter performance as shown in Fig. 2. The common source inductance, L_s, is the inductance shared by the drain-to-source power current path and gate driver loop. The high frequency power loop inductance, L_{Loop}, is the inductance in the device commutation loop, which is comprised of the parasitic inductance from the positive terminal of the input capacitance, through the top device, synchronous rectifier, ground loop, and input capacitor.

The common source inductance, L_s, has been shown to be critical to performance because it directly impacts the driving speed of the devices [8],[9]. As common source inductance increases, the effective gate drive voltage and gate drive current are significantly reduced, slowing switching speeds and increasing switching losses as described in equation (1). The impact of common source inductance on a switching transition can be seen as part of the parasitic di/dt voltage bump on the Si MOSFET waveform shown in Fig. 2. The available gate drive current at turn-on is given by:

$$I_G = \frac{V_{Driver} - V_{GS} - V_{L_S}}{R_G} = \frac{V_{Driver} - V_{GS} - L_S \cdot \frac{di_{DS}}{dt}}{R_G} \quad (4)$$

Where V_{Driver} is gate drive voltage, V_{GS} is the gate to source voltage across the device, V_{LS} is the effective voltage across the common source inductance, which is equal to $L_S \cdot di_{DS}/dt$ during device current commutation, and R_G is the effective gate resistance including the driver resistance, the internal power device resistance, and external gate loop resistance.

The high frequency loop inductance, L_{Loop}, while not as penalizing to switching speeds as common source inductance, still negatively impacts switching performance [4],[10]-[12]. Another major drawback of high frequency loop inductance is the drain-to-source voltage spike induced during the switching transition, shown in Fig. 2, given by:

$$V_{L_{LOOP}} = L_{LOOP} \cdot \frac{di_{DS}}{dt} \quad (5)$$

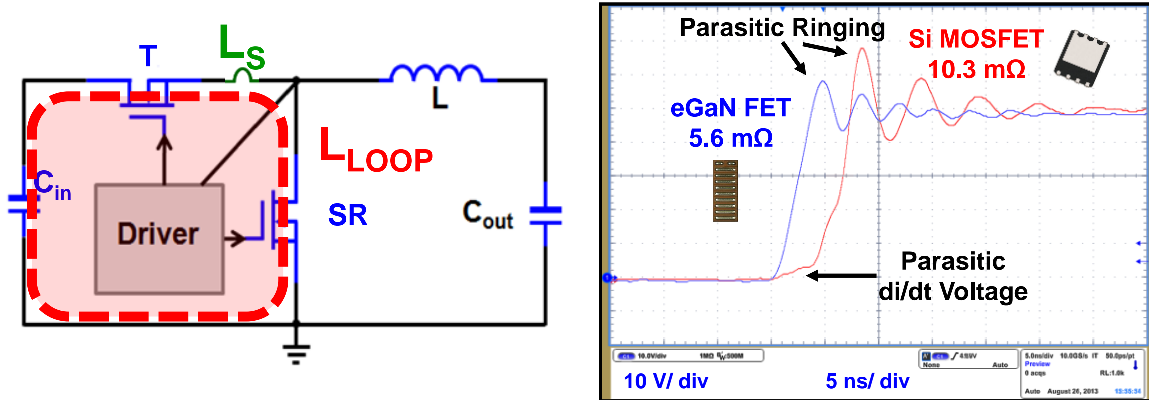

Fig. 2. Synchronous buck converter with parasitic inductances and switching node waveforms of eGaN FET and MOSFET designs (V_{IN}=48 V, I_{OUT}=10 A, f_{sw}=300 kHz, GaN transistors: EPC2001 MOSFETs: BSZ123N08NS3G).

3.1 Package Parasitics

To enable the high switching speed available from the low FOM of GaN transistors, low parasitic packaging and printed circuit board (PCB) layout is required. This subsection will compare the device packaging of GaN transistors and Si MOSFETs.

For Si trench MOSFET structures, the gate and source terminals and the drain terminal are located on opposite sides of the device. This forces an external connection from either the source and gate or the drain to connect the device to the PCB, introducing performance limiting package parasitics. The Loss Free Package (LFPAK), one of the most common packages for Si devices, is shown on the left in Fig. 3. The LFPAK uses an external lead frame to connect the source and gate terminals to the PCB. The source connection of the LFPAK introduces over 0.5 nH of common source inductance alone, degrading the in-circuit performance of the Si power device [3].

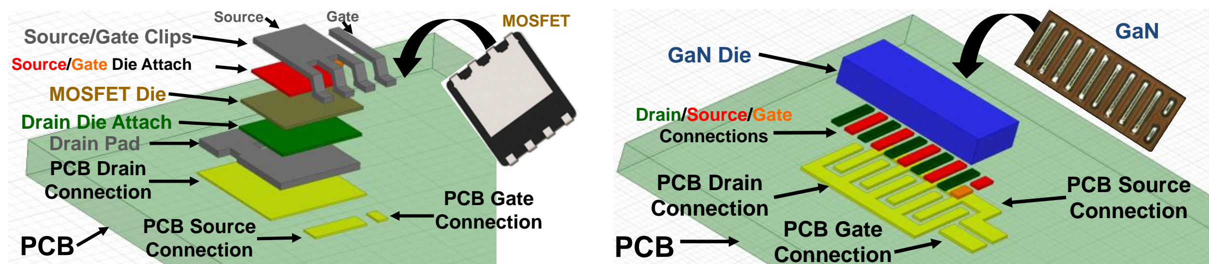

Fig. 3. Exploded view of packages for Si Loss Free Package (left) GaN Land Grid Array (right).

The high voltage lateral GaN transistor in a Land Grid Array (LGA) package has a major packaging advantage because all of the connections are located on the same side of the die, as shown on the right of Fig. 3, eliminating the requirement of complex high-parasitic packaging. The LGA GaN transistor has a total package inductance estimated to be under 0.2 nH, significantly lower than any Si MOSFET package. In [3], the impact of the GaN transistor LGA package and the reduction of package parasitic inductance and resistance over the best available trench devices are quantified.

3.2 Printed Circuit Board Parasitics

With higher switching speeds and lower package parasitic inductances the printed circuit board layout can become the limiting factor in converter performance. The most critical parasitic to reduce is the common source inductance, which is the inductance shared by the high frequency power loop and gate driver loop. To minimize the common source inductance added by PCB layout it is recommended to locate the gate driver loop and high frequency power loop where they have very little interaction. An example layout is shown in Fig. 4, where the gate drive loop, shown in red, and the high frequency loop, shown in yellow, interact only directly next to the GaN transistor, minimizing the common source inductance to the ultra-low internal package inductance offered by the GaN transistor package.

To reduce the loop inductance over conventional designs an optimal layout was developed that utilizes the first inner layer, shown in the bottom left of Fig. 4, as a power loop return path. This return path is located directly underneath the top layer's power loop path, shown in the upper left of Fig. 4, allowing for the smallest physical loop size and providing magnetic field self-cancellation. The side view, shown in Fig. 4 illustrates the concept of creating a low profile magnetic field self-cancelling loop in a multilayer PCB structure. By using the optimal layout developed by EPC, GaN based half bridge designs have achieved high frequency loop inductances below 0.4 nH [4], further improving the in-circuit performance of GaN transistors when compared to Si MOSFETs.

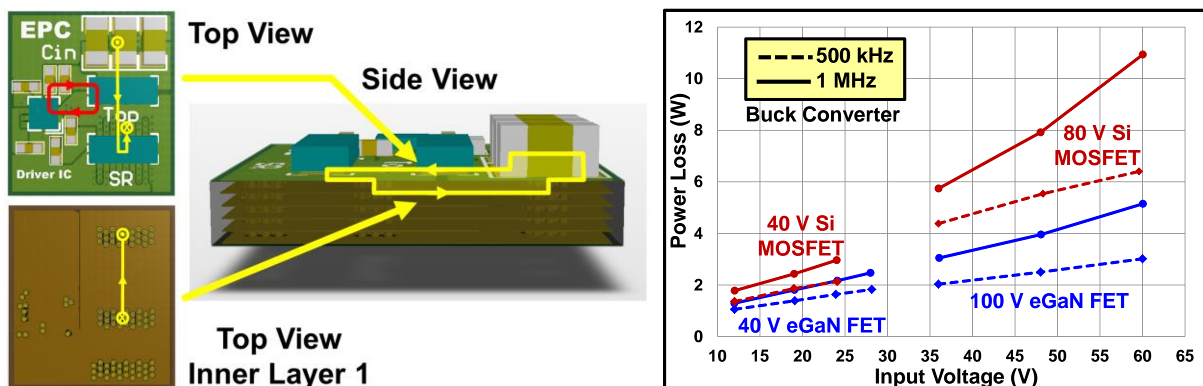

Fig. 4. Optimal power loop with GaN transistors, top view, top view of inner layer 1, and side view (left). Experimental power loss comparisons for GaN transistors and Si MOSFETs in synchronous buck converter (right) (V_{OUT}=1.2 V, 40 V GaN transistors T/SR: EPC2015, 40 V Si MOSFETS T: BSZ097N04LSG SR: BSZ040N04LSG, 100 V GaN transistors T/SR: EPC2001, 80 V MOSFETS T/SR: BSZ123N08NS3G).

Combining lower FOM, lower package parasitics, and lower parasitic PCB layouts, GaN transistors provide significant performance benefits over state of the art Si technology. GaN transistors have the ability to improve switching speeds with lower on-resistance devices as shown on the right of Fig. 2. This allows for circuit designers to achieve lower dynamic switching losses and lower static conduction losses. This leads to lower loss designs as shown on the right in Fig. 4, which contains a plot of power loss for experimental synchronous buck converters with input voltages ranging from 12 V to 60 V operating at switching frequencies of 500 kHz and 1 MHz. The GaN transistors provide improved performance in all cases, with the benefits increasing with frequency and voltage. GaN transistors allow increased switching frequencies without sacrificing performance.

4. Improving High Speed GaN Transistors Parallel Performance

The previous sections demonstrated enhanced performance with single GaN transistors. In many applications, higher current is required. In this section, we will evaluate the ability to parallel GaN transistors to provide high efficiency in high output current applications.

4.1 Challenges of Paralleling High Speed GaN Transistors

The objective of paralleling devices is to combine multiple higher on-resistance devices to appear and operate as a single, lower on-resistance device allowing for higher power handling capability. To effectively parallel devices, each device should equally share current dynamically, and in steady state, and equally divide switching related losses. The introduction of unbalanced in-circuit parasitics between parallel devices leads to uneven sharing and degraded electrical and thermal performance, limiting the effectiveness of paralleling devices [13]. For high speed devices such as GaN transistors, the increased switching speeds amplify the impact of parasitic mismatches [14].

In the previous section, the importance of minimizing common source inductance and high frequency loop inductance were addressed. For paralleling GaN transistors, these parasitics must not only be minimized to achieve the best performance but also need to be balanced to ensure proper parallel operation. The graph on the left of Fig. 5 shows the impact of parasitic imbalance in the high frequency loop inductance for two parallel GaN half bridges operating at 48 V with various common source inductances. As the difference between the high frequency loop inductance increases between the parallel half bridges, so does the dynamic current difference:

$$I_{DIFF} = \frac{I_{SW1} - I_{SW2}}{I_{SW1} + I_{SW2}} \qquad (6)$$

Where I_{DIFF} is the dynamic current difference between the two parallel GaN half bridges and I_{SW1} and I_{SW2} are the respective currents in the parallel transistors when the output current (I_{OUT}) is reached after a switching transition.

From the left graph in Fig. 5 it can also be observed that as the common source inductance decreases, current sharing issues become more pronounced. The magnified current sharing issues at lower common source inductance is caused by the higher switching speeds achieved as common source inductance decreases. As the current sharing worsens between parallel devices the electrical and thermal performance degrades as we will show in section 4.2.

The current sharing difference resulting from parasitic imbalance in the common source inductance for two parallel GaN half bridges operating at 48 V for various high frequency loop inductances (L_D=L_{LOOP}-L_S) is shown on the right in Fig. 5. Similar to loop inductance imbalance, as common source inductance varies, current sharing worsens. This trend is magnified as loop inductance decreases and capable switching speeds increase.

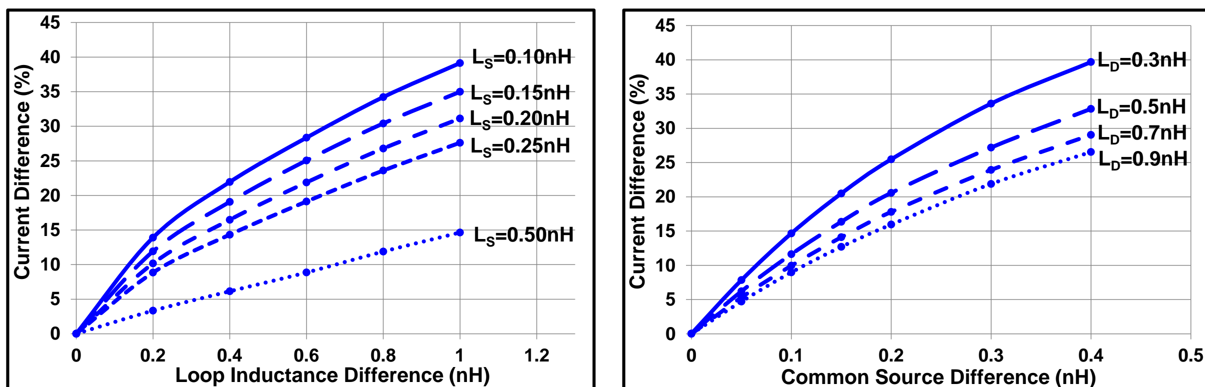

Fig. 5. Impact of high frequency loop inductance (left) and common source inductance (right) parasitic imbalance on device dynamic current sharing for a V_{IN}=48 V, I_{OUT}=25 A, single phase GaN based buck converter with two half bridges operating in parallel (GaN transistors: EPC 2001).

4.2 Optimizing Parallel PCB Layout

As switching speeds steadily increase and parasitic inductances continue to decrease, improved techniques must be developed to improve parallel performance. To effectively parallel high speed GaN transistors the parasitic imbalance contributed by the PCB layout must be minimized. We will look at two different parallel layouts based on the optimal layout discussed in section 3.2 and assess their ability to provide parallel performance similar to an optimized single transistor design. Each half bridge design contains four devices in parallel for the top switch (T1-4) and synchronous rectifier (SR1-4) and was tested in a single phase buck converter configuration from 48 V to 12 V at a switching frequency of 300 kHz. In total, eight 100 V EPC2001 GaN transistors with a single TI LM5113 gate driver were used to achieve output power up to 480 W and output currents up to 40 A.

The parallel designs are shown in Fig. 6; with the first design on the left using an expansion of the optimal layout shown in Fig. 4. In the first design, the four GaN transistors are located in close proximity to operate as a "single" power device, with a single high frequency power loop. The drawbacks of this layout are that the high frequency loop inductance will increase as a result of the increased loop size and that devices will have imbalanced parasitics as their individual power loops are different (L_{LOOP}≈1.7-2.6 nH); leading to current sharing and thermal issues. The second design, shown on the right in Fig. 6 utilizes four distributed high frequency power loops, located symmetrically around the single LM5113 gate driver. The design will provide the lowest overall parasitics for each device pair (L_{LOOP}≈0.4 nH) and most importantly, provide the best balancing of the parasitic elements, ensuring proper parallel operation.

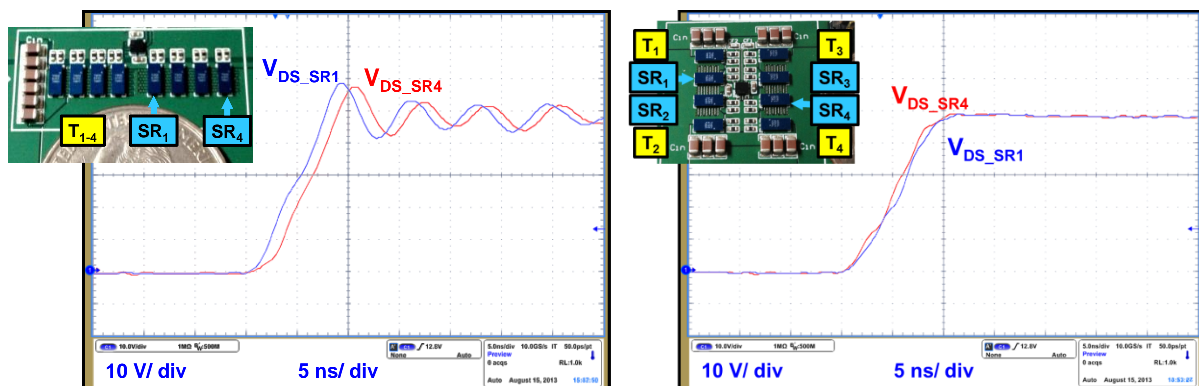

Fig. 6. Four parallel GaN half bridge layouts and switching node waveforms with a single high frequency power loop (left) and four distributed high frequency power loops (right) (V_{IN}=48 V, V_{OUT}= 12 V, I_{OUT}=30 A, f_{sw}=300 kHz, GaN transistors T/SR: EPC2001).

The voltage waveforms of the synchronous rectifiers switching transitions for the two designs are also shown in Fig. 6. For the single high frequency power loop design, the switching node waveforms are shown on the left in Fig. 6, the voltage transitions for the inner-most and outer-most devices show an almost 2 ns switching time difference, which equates to about 25% of the total switching time. This voltage difference demonstrates the parasitic imbalance in this PCB layout. For the symmetrical four high frequency power loop design the switch-node waveforms are shown on the right in Fig. 6. The voltage transitions for the devices are almost identical, demonstrating this layout's ability to balance the parasitics well. This balanced layout will improve overall performance by offering better electrical and thermal performance.

The thermal evaluation of the two designs, shown in Fig. 7, demonstrates the thermal imbalance of the single high frequency loop design. The left image in Fig. 7 shows a hot spot developing on the devices handling a greater portion of the power as a result of parasitic imbalance. The top switch closest to the input capacitors, T1, has a maximum temperature more than 10°C higher than the top switch furthest away from the input capacitors, T4. For the four distributed power loop design, shown on the right in Fig. 7, there is a very good

thermal balance, with negligible difference in temperature between devices and a good distribution of the heat by avoiding clustering of the higher loss top devices on the PCB.

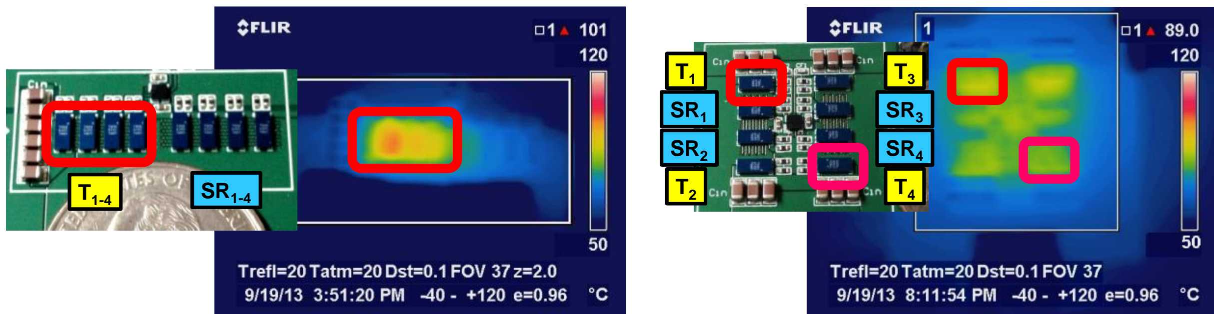

Fig. 7. Thermal measurements of parallel GaN half bridge layouts with a single high frequency power loop (left) and four distributed high frequency power loops (right). (V_{IN}=48 V, V_{OUT}=12 V, I_{OUT}=30 A, f_{sw}=300 kHz, L=3.3 μH, GaN transistors T/SR: 100 V EPC2001, fan speed: 200 LFM).

By offering lower individual parasitics and better parasitic balance, the distributed four high frequency loop design has more effective paralleling. This results in better electrical and thermal performance as shown in Fig. 8. The distributed high frequency loop design offers a 0.2% gain in efficiency at 40 A, and has an almost constant 10° C improvement in the maximum device temperature.

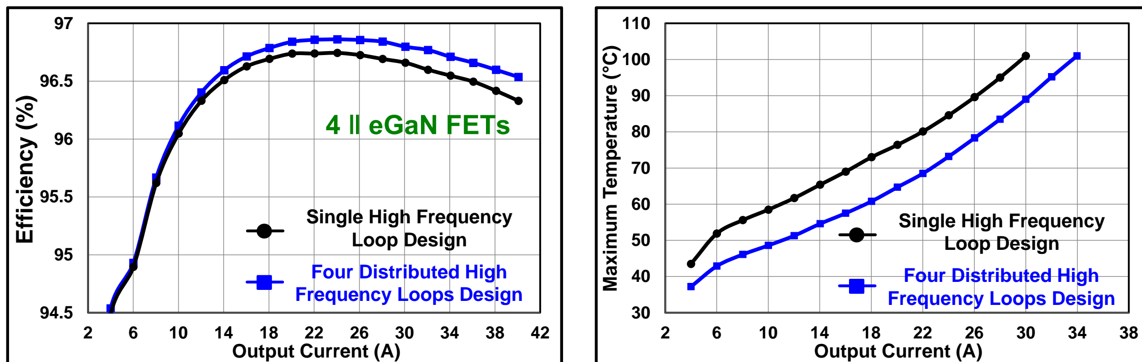

Fig. 8. Efficiency (left) and thermal comparison (right) for conventional and proposed parallel GaN half bridge designs (V_{IN}=48 V, V_{OUT}=12 V, f_{sw}=300 kHz, L=3.3 uH, GaN transistors T/SR: EPC2001).

The switching waveforms for an optimal PCB design with a single GaN transistor, two parallel transistors, and four parallel transistors are shown in Fig. 9. Looking at the entire switching cycle, as shown on the left in Fig. 9, the switching speed difference is unnoticeable, demonstrating the ability of parallel GaN transistors to offer high switching speeds for high current applications. Looking at a zoomed view of the switching rise time, as shown on the right in Fig. 9, the parallel designs effectively operate as a single, larger, lower-resistance device with a slower switching speed in proportion to the number of devices in parallel.

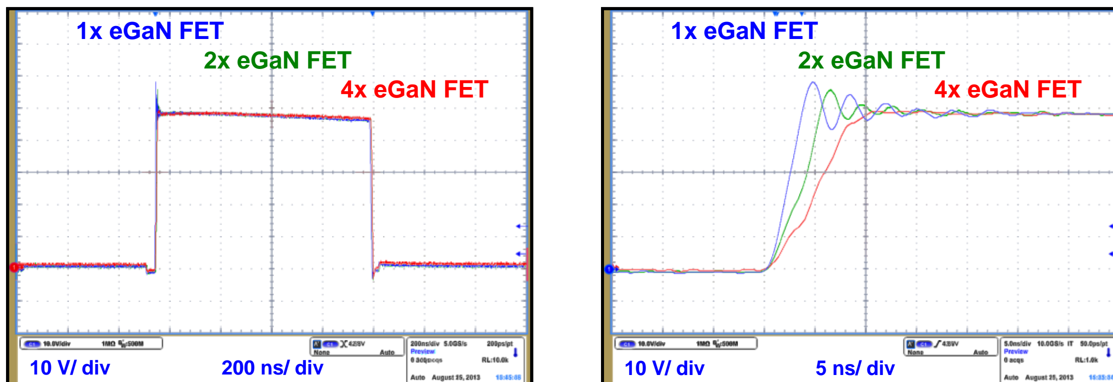

Fig. 9. Switching node waveforms with 1, 2 and 4 parallel GaN half bridges (left), zoomed view (right) (V_{IN}=48 V, V_{OUT}=12 V, I_{OUT}=30 A/number of GaN FETs, f_{sw}=300 kHz, GaN FET T/SR: 100 V EPC2001).

5. Conclusions

The introduction of high performance GaN transistors offers the potential to switch at higher frequencies and efficiency than possible with traditional Si MOSFET technology. Combined with improved figures of merit and low parasitic packaging, GaN transistors require a low parasitic PCB layout to fully utilize the device's capability. This work addressed the impact of package and layout parasitics on in-circuit performance and proposed an optimized layout to further enhance the performance capability of GaN transistors. This paper then evaluated the ability to parallel GaN transistors for higher output current applications by addressing the challenges facing paralleling high speed, low parasitic devices and proposing an improved paralleling technique. For experimental verification of the proposed design method, four parallel half bridges in an optimized layout were operated as a 48 V to 12 V, 480 W, 300 kHz, 40 A single phase buck converter and achieved efficiencies above 96.5% from 35% to 100% load. The proposed design achieved superior electrical and thermal performance compared to conventional paralleling methods and demonstrated that high speed GaN transistors can be effectively paralleled for higher current operation.

6. References

[1] A. Lidow, J. Strydom, M. de Rooij, and Y. Ma, GaN Transistors for Efficient Power Conversion, 1rst edition, El Segundo, Ca, 2012.

[2] N. Ikeda, S. Kaya, L. Jiang, Y. Sato, S. Kato, and S. Yoshida, "High Power AlGaN/GaN HFET with a High Breakdown Voltage of Over 1.8 kV on 4 Inch Si Substrates and the Suppression of Current Collapse," Power Semiconductor Devices and IC's (ISPSD), pp.287-290, 2008.

[3] D. Reusch, D. Gilham, Y. Su, and F. C. Lee, "Gallium Nitride Based 3D Integrated Non-Isolated Point of Load Module," Applied Power Electronics Conference and Exposition (APEC), pp. 38 –45, 2012.

[4] D. Reusch and J. Strydom, "Understanding the Effect of PCB Layout on Circuit Performance in a High Frequency Gallium Nitride Based Point of Load Converter," Applied Power Electronics Conference and Exposition (APEC), pp.649-655, 2013.

[5] A. Q. Huang, "New Unipolar Switching Power Device Figures of Merit," IEEE Electron Device Letters, vol. 25, pp. 298-301, 2004.

[6] B. J. Baliga, "Power semiconductor device Figure-of-merit for high frequency applications," IEEE Electron Device Letters, vol. 10, pp. 455–457, 1989.

[7] D. Reusch, J. Strydom, and A. Lidow, "Improving System Performance with eGaN® FETs in DC-DC Applications," International Microelectronics Assembly and Packaging Society (IMAPS), pp.764-769, 2013.

[8] B. Yang, J. Zhang, "Effect and utilization of common source inductance in synchronous rectification," Applied Power Electronics Conference and Exposition (APEC), pp. 1407–1411, 2005.

[9] M. Pavier, A. Woodworth, A. Sawle, R. Monteiro, C. Blake, and J. Chiu, "Understanding the effect of power MOSFET package parasitic on VRM circuit efficiency at frequencies above 1 MHz," PCIM Europe, pp. 279–284, 2003.

[10] T. Hashimoto, T. Kawashima, T. Uno, Y. Satou, N. Matsuura, "System in package with mounted capacitor for reduced parasitic inductance in voltage regulators," Applied Power Electronics Conference and Exposition (APEC), pp.187-191, 2008.

[11] D. Reusch, F.C. Lee, Y. Su, D. Gilham, "Optimization of a High Density Gallium Nitride Based Non-Isolated Point of Load Module," Energy Conversion Congress and Exposition (ECCE), pp. 2914-2920, 2012.

[12] D. Reusch, "High Frequency, High Power Density Integrated Point of Load and Bus Converters," PhD Dissertation, Virginia Tech, 2012.

[13] J. B. Forsythe, "Paralleling of Power MOSFETs for High Power Output," International Rectifier Application Note.

[14] Y. F. Wu, "Paralleling High-speed GaN Power HEMTs for Quadrupled Power Output," Applied Power Electronics Conference and Exposition (APEC), pp. 211-214, 2013.